

Self-frequency blueshift of dissipative solitons in silicon-based waveguides

Citation for published version:

Roy, S, Marini, A & Biancalana, F 2013, 'Self-frequency blueshift of dissipative solitons in silicon-based waveguides', *Physical Review A*, vol. 87, no. 6, 065803. <https://doi.org/10.1103/PhysRevA.87.065803>

Digital Object Identifier (DOI):

[10.1103/PhysRevA.87.065803](https://doi.org/10.1103/PhysRevA.87.065803)

Link:

[Link to publication record in Heriot-Watt Research Portal](#)

Document Version:

Publisher's PDF, also known as Version of record

Published In:

Physical Review A

General rights

Copyright for the publications made accessible via Heriot-Watt Research Portal is retained by the author(s) and / or other copyright owners and it is a condition of accessing these publications that users recognise and abide by the legal requirements associated with these rights.

Take down policy

Heriot-Watt University has made every reasonable effort to ensure that the content in Heriot-Watt Research Portal complies with UK legislation. If you believe that the public display of this file breaches copyright please contact open.access@hw.ac.uk providing details, and we will remove access to the work immediately and investigate your claim.

Self-frequency blueshift of dissipative solitons in silicon-based waveguides

Samudra Roy,¹ Andrea Marini,¹ and Fabio Biancalana^{1,2}

¹Max Planck Institute for the Science of Light, Günther-Scharowsky-Straße 1, 91058 Erlangen, Germany

²School of Engineering & Physical Sciences, Heriot-Watt University, EH14 4AS Edinburgh, United Kingdom

(Received 22 May 2013; published 27 June 2013)

We analyze the dynamics of dissipative solitons in silicon on insulator waveguides embedded in a gain medium. The optical propagation is modeled through a cubic Ginzburg-Landau equation for the field envelope coupled with an ordinary differential equation accounting for the generation of free carriers owing to two-photon absorption. Our numerical simulations clearly indicate that dissipative solitons accelerate due to the carrier-induced index change and experience a considerable blueshift, which is mainly hampered by the gain dispersion of the active material. Numerical results are fully explained by analytical predictions based on soliton perturbation theory.

DOI: [10.1103/PhysRevA.87.065803](https://doi.org/10.1103/PhysRevA.87.065803)

PACS number(s): 42.65.Tg, 42.65.Sf, 42.65.Wi

Silicon photonics has attracted considerable attention among researchers owing to its potential applications ranging from optical interconnection to biosensing. In the last few years, silicon-on-insulator (SOI) technology has rapidly developed into a well-established photonic platform [1]. The tight confinement of the optical mode and the inherently large bulk nonlinearity of Si tremendously enhance the nonlinear dynamics [2]. For near-infrared wavelengths in the range $1 \mu\text{m} < \lambda_0 < 2.2 \mu\text{m}$, two-photon absorption (2PA) is the leading loss mechanism and limits the spectral broadening due to self-phase modulation (SPM) [3]. As a consequence of 2PA, electrons are excited to the conduction band, absorb light, and affect the pulse dynamics by modifying the refractive index of silicon [4]. Loss mechanisms are restricted in silicon-organic hybrid slot waveguides, which can be exploited for all-optical high-speed signal processing [5]. Alternatively, loss can be overcome by embedding active materials in the design of SOI devices. Recently, some amplification schemes based on III-V semiconductors, rare-earth-ion-doped dielectric thin films, and erbium-doped waveguides have been proposed and realized [6,7].

In this paper, we describe the nonlinear dynamics of dissipative solitons (DSs) in amplifying SOI devices. DSs are stationary localized structures of open nonlinear systems far from equilibrium that can be observed in several contexts [8]. Analogously to SOI waveguides, also in plasmonics loss mechanisms are relevant and spatial DSs have been proposed to achieve self-induced lateral confinement [9]. Although the model considered in our analysis is general and can be applied to any silicon-based amplifying setup, we specialize our calculations to a SOI waveguide embedded in Er-doped amorphous aluminium oxide ($\text{Al}_2\text{O}_3:\text{Er}^+$). Other gain schemes involving the use of semiconductor active materials can also be considered and gain dispersion can be reduced accordingly. For the representative structure displayed in Fig. 1, the gain bandwidth is of the order of 100 nm around the carrier wavelength $\lambda \simeq 1540$ nm. For this waveguide, the second-order group velocity dispersion (GVD) coefficient and the effective area at $\lambda_0 = 1550$ nm are calculated to be $\beta_2 \simeq -2 \text{ ps}^2/\text{m}$ and $A_{\text{eff}} \simeq 0.145 \mu\text{m}^2$, respectively. The proposed SOI waveguide is fabricated along the $[110]$ direction and on the $[110] \times [001]$ surface, so that quasi-TM modes do not experience stimulated Raman scattering (SRS) [4]. The propagation of an optical pulse with envelope $u(z, t)$ and carrier frequency ω_0 in the proposed photonic structure is governed

by a complex Ginzburg-Landau (GL) equation,

$$i\partial_\xi u - \frac{1}{2}\text{sgn}(\beta_2)\partial_\tau^2 u + i\alpha u + (1 + iK)|u|^2 u + (i/2 - \mu)\phi_c u - i(g + g_2\partial_\tau^2)u = 0, \quad (1)$$

coupled with an ordinary differential equation accounting for the 2PA-induced free-carrier dynamics $d\phi_c/d\tau = \theta|u|^4 - \tau_c\phi_c$ [4]. Equation (1) is written in dimensionless units, where the time (t) and the longitudinal spatial variable (z) are normalized to the initial pulse width ($t = t_0\tau$) and to the dispersion length ($z = \xi L_D$ with $L_D = t_0^2/|\beta_2(\omega_0)|$), respectively. The envelope amplitude (A) is rescaled to $A = u\sqrt{P_0}$, where $P_0 = |\beta_2(\omega_0)|/(t_0^2\gamma_R)$, $\gamma_R = k_0 n_2/A_{\text{eff}}$, and $n_2 \simeq (4 \pm 1.5) \times 10^{-18} \text{ m}^2/\text{W}$ is the Kerr nonlinear coefficient of bulk silicon. The bulk 2PA coefficient is $\beta_{2\text{PA}} \simeq 8 \times 10^{-12} \text{ m/W}$ and its corresponding effective waveguide counterpart $\gamma_I = \beta_{2\text{PA}}/(2A_{\text{eff}})$ is rescaled to the Kerr coefficient so that $K = \gamma_I/\gamma_R = \beta_{2\text{PA}}\lambda_0/(4\pi n_2)$. The linear loss coefficient (α_l) is renormalized to the dispersion length ($\alpha = \alpha_l L_D$) and can be neglected for short propagation in the linear transparency spectral window of silicon, $1 \mu\text{m} < \lambda_0 < 10 \mu\text{m}$, where 2PA dominates (if $\lambda_0 < 2.2 \mu\text{m}$). The density of free-carriers (FCs) N_c generated through 2PA is normalized so that $\phi_c = \sigma N_c L_D$, where $\sigma \simeq 1.45 \times 10^{-21} \text{ m}^2$, the free-carrier absorption (FCA) cross section of Si at $\lambda_0 = 1.55 \mu\text{m}$ [10]. FCs are responsible for FCA regulated by the parameter $\theta = \beta_{2\text{PA}}|\beta_2|\sigma/(2\hbar\omega_0 A_{\text{eff}}^2 t_0 \gamma_R^2)$ [11] and free-carrier dispersion (FCD) depending on the parameter $\mu = 2\pi k_c/(\sigma\lambda_0)$, where $k_c \simeq 1.35 \times 10^{-27} \text{ m}^3$ [12]. The parameter θ has a significant implication in the context of the present problem where we are investigating the carrier-mediated frequency blueshift. The generation rate of FCs is governed by θ , which depends on the waveguide features and on external parameters, e.g., operating frequency and input pulse width. A larger value of θ can produce more blueshift but at the same time it increases the FCA loss. We calculated θ with the realistic parameters of the SOI waveguide shown in Fig. 1, but in principle this value can be modified by using a different waveguide structure. t_c is the characteristic FC recombination time (of the order of nanoseconds) and normalized as $\tau_c = t_0/t_c$. In the following calculations we neglect the recombination term, since we focus our analysis on ultrashort pulses with a time duration of the order $t_0 \simeq 100$ fs. The amplifying medium is characterized by a gain coefficient, G , which in our dimensionless equations is

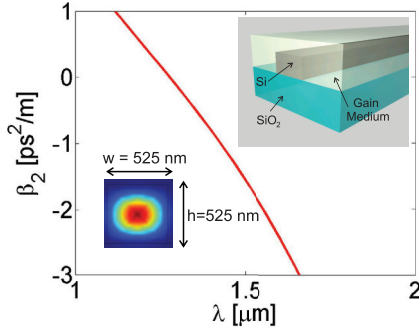


FIG. 1. (Color online) Sketch of a SOI waveguide with lateral dimensions $h = w = 525$ nm surrounded by $\text{Al}_2\text{O}_3:\text{Er}^+$ and its dispersion property. The solid red line represents the GVD of the quasi-TM mode, whose spatial profile at $\lambda_0 = 1550$ nm is depicted in the inset below.

rescaled to the dispersion length ($g = GL_D$), and a dephasing time, T_2 , which is related to the dimensionless gain dispersion coefficient through $g_2 = g(T_2/t_0)^2$.

The presence of gain and 2PA in the photonic structure considered in our calculations implies that, in general, energy is not conserved. Nevertheless, the GL equation supports isolated stationary solitons where overall gain and loss are balanced. In contrast to Kerr solitons in conservative systems, which form continuous families of localized solutions, DSs are formed under a strict dynamical equilibrium involving nontrivial internal energy flows. In turn, DSs are associated with certain discrete parameters of the GL equation that satisfy the energy balance condition. In absence of linear loss (i.e., $\alpha = 0$) and FCs (i.e., $\phi_c = 0$), DSs can be found as

$$u(\xi, \tau) = u_0 [\text{sech}(\eta\tau)]^{1-i\beta} e^{i\Gamma\xi}, \quad (2)$$

where the parameters u_0 , η , β , and Γ satisfy the following relations:

$$|u_0|^2 = \frac{\eta^2}{K} \left[\text{sgn}(\beta_2) \frac{3}{2} \beta - g_2(2 - \beta^2) \right], \quad (3)$$

$$\eta^2 = \frac{g}{\{\beta[\Theta g_2 + \text{sgn}(\beta_2)] + g_2\}}, \quad (4)$$

$$\beta_{\pm} = \frac{\Theta}{2} \pm \left[\left(\frac{\Theta}{2} \right)^2 + 2 \right]^{1/2}, \quad (5)$$

$$\Gamma = \text{sgn}(\beta_2) \frac{\eta^2}{2} (\beta^2 - 1) - 2\beta g_2 \eta^2, \quad (6)$$

$$\Theta = \frac{6g_2 K + \text{sgn}(\beta_2) 3}{\text{sgn}(\beta_2) K - 2g_2}. \quad (7)$$

Note that the exact values of u_0 , η , β , and Γ are fixed by the physical parameters of the system: g , g_2 , and K [8]. It is well known that solitons of the cubic GL equation suffer from inherent core and background instabilities [13], which generate bifurcations and chaotic states [14,15]. In principle, DSs can be stabilized by introducing higher-order nonlinearities or by coupling the system to a passive waveguide [16,17], but this task goes beyond the scope of the present work, where we aim at understanding the effect of FCs on the DS dynamics. In order

to grasp the fundamental effects induced by FC dynamics, we develop a soliton perturbative analysis [18], approximating the GL equation as a perturbed nonlinear Schrödinger equation (NLSE): $i\partial_{\xi}u + \frac{1}{2}\partial_{\tau}^2u + |u|^2u = i\epsilon(u)$, where we explicitly consider the case of anomalous dispersion ($\beta_2 < 0$) and $\epsilon(u)$ includes the coupling to FCs, 2PA, linear gain, and its dispersion: $\epsilon = (g - K|u|^2 - \phi_c/2 - i\mu\phi_c + g_2\partial_{\tau}^2)u$. The perturbative theory is developed by making the ansatz

$$u(\xi, \tau) = u_0(\xi) (\text{sech}\{\eta(\xi)[\tau - \tau_p(\xi)]\})^{1-i\beta} e^{i\phi(\xi) - i\Omega(\xi)[\tau - \tau_p(\xi)]}, \quad (8)$$

where the parameters u_0 , η , τ_p , ϕ , and Ω are now assumed to depend on ξ and $\epsilon(u)$ is considered as a small perturbation depending on u and u^* and their derivatives. The perturbation technique aims at obtaining the evolution dynamics of each individual parameter over the propagation distance. Introducing the Lagrangian density and integrating it over τ , one gets the total Lagrangian in the following form:

$$L = 2u_0^2\eta^{-1}(\partial_{\xi}\phi + \Omega\partial_{\xi}\tau_p) + \beta u_0^2\eta^{-2}\partial_{\xi}\eta + \eta u_0^2(1 + \beta^2)/3 + u_0^2\eta^{-1}(\Omega^2 - 2u_0^2/3) + i \int_{-\infty}^{\infty} (\epsilon u^* - \epsilon^* u) d\tau. \quad (9)$$

In turn, from the Lagrangian above one can derive the reduced Euler-Lagrangian equations for the pulse parameters [19]. This procedure leads to a set of differential equations accounting for the soliton dynamics. We here focus on the evolution of the pulse energy ($E = \int_{-\infty}^{\infty} |u|^2 d\tau$), frequency (Ω), and temporal position (τ_p). The evolution of these three parameters is derived by the standard variational technique [19,20]

$$\frac{dE}{d\xi} = \frac{d}{d\xi} \left(\frac{2u_0^2}{\eta} \right) = \text{Re} \int_{-\infty}^{\infty} \epsilon u^* d\tau, \quad (10)$$

$$\frac{d\Omega}{d\xi} = -\frac{\eta^2}{u_0^2} \int_{-\infty}^{\infty} \tanh[\eta(\tau - \tau_p)] \text{Re}[(\beta - i)\epsilon u^*] d\tau, \quad (11)$$

$$\frac{d\tau_p}{d\xi} = -\delta + \frac{\eta}{u_0^2} \int_{-\infty}^{\infty} (\tau - \tau_p) \text{Re}(\epsilon u^*) d\tau, \quad (12)$$

where Re and Im stand for real and imaginary parts. Taking the integrations involving the perturbation ϵ one can find

$$\frac{dE}{d\xi} = -2E \left(\frac{1}{6} \theta u_0^2 E + g_2 \Omega^2 \right), \quad (13)$$

$$\frac{d\Omega}{d\xi} = \frac{8}{15} (\mu + \beta/2) \theta u_0^4 - \frac{4}{3} g_2 (1 + \beta^2) \Omega \eta^2, \quad (14)$$

$$\frac{d\tau_p}{d\xi} = -(1 - 2g_2\beta)\Omega - \frac{7}{72} \theta E^2. \quad (15)$$

The perturbative analysis reveals that FCs induce frequency blueshift and temporal acceleration of DSs, both effects being hampered by the gain dispersion that limits blueshifting within the amplifying frequency window of the active material. We emphasize that the energy is reduced only by FCA and gain dispersion, since 2PA is initially thoroughly balanced by the external gain. For small gain dispersion, Eq. (14) is solved analytically with the initial condition $\Omega(0) = 0$, obtaining $\Omega(\xi) \approx f\xi$, where $f = 8(\mu + \beta/2)\theta u_0^4/15$. This expression predicts that DSs experience a spectral blueshift proportional to the propagation distance through a rate (f) that basically depends on the FC density and peak amplitude. Under the assumption of small energy decrease ($E \approx \text{constant}$), which

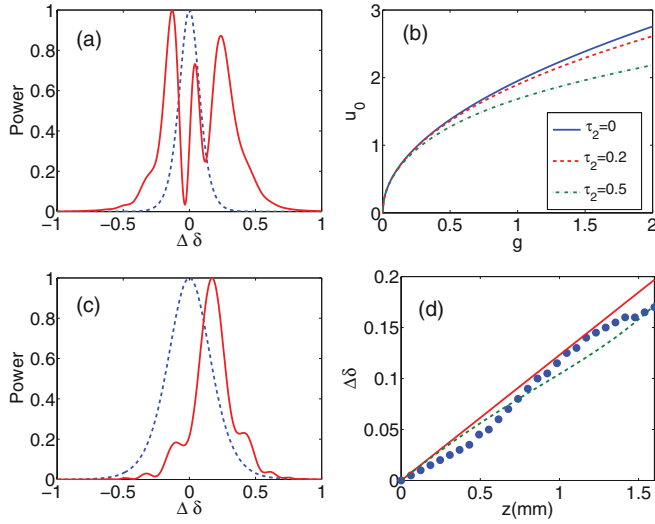


FIG. 2. (Color online) (a) Asymmetric spectral broadening of the NLSE soliton ($u_{in} = \text{sech}\tau$) with time duration $t_0 = 40$ fs for $g = 1$ and $g_2 = 0$ at $\xi = 2$. (b) DS amplitude u_0 as a function of linear gain g for several dephasing times ($\tau_2 = T_2/t_0 = 0, 0.2, 0.5$) at fixed K . (c) Carrier-induced blueshift of DS ($u_{in} = u_0[\text{sech}(\eta\tau)]^{1-i\beta}$) for the same parameters of panel (a), where $u_0 = \sqrt{3g/(2K)}$, $\eta = \sqrt{-g/\beta}$, and $\beta = 3/(2K) - \sqrt{[3/(2K)]^2 + 2}$. Solid red and blue dashed lines indicate the output and input power spectra, respectively. (d) z -dependent DS frequency shift [$\Delta\delta = \Omega/(2\pi)$] for $g_2 = 0$. Perturbative predictions with constant (solid red line) and z -dependent (green dotted line) peak amplitude u_0 are shown. The solid blue dots indicate numerical findings.

is true only for small propagation distance, the solution of the temporal shift can be approximated as

$$\tau_p(\xi) \approx -(a\xi + f\xi^2/2), \quad (16)$$

where $a = 7\theta E^2/72$. The equation above suggests that during propagation DSs are accelerated under the influence of FCDs analogously to the recently studied case of optical solitons in gas-filled hollow-core photonic crystal fibers [18].

In Fig. 2(a) we show the conventional asymmetric spectral broadening of NLSE solitons [21]. In Fig. 2(b) we plot the DS amplitude (u_0) as a function of linear gain for several dephasing times ($\tau_2 = T_2/t_0 = 0, 0.2, 0.5$). As shown in Fig. 2(c), even though DSs of the cubic GL equation are unstable, they experience a considerable carrier-induced blueshift maintaining their shape over a propagation distance of the order of millimeters. Indeed, for DSs, 2PA is exactly compensated by the linear gain, while NLSE solitons experience an imbalanced dynamical evolution due to 2PA and amplification. In Fig. 2(d) we compare the perturbatively predicted FC-induced frequency blueshift (solid red and dashed green lines) with numerical results (solid blue dots), finding that, for the initial part of pulse propagation, perturbative predictions nicely match with the numerical findings. The dimensionless frequency shift is calculated to be $\Delta\delta \simeq 0.16$ at $\xi = 2$, corresponding in physical units to $\Delta\lambda \simeq 35$ nm. The solid red line in Fig. 2(d) represents the predicted frequency shift calculated through the perturbation analysis by approximating the DS amplitude to remain constant, whereas the green dotted line represents the perturbative prediction considering z -dependent DS amplitudes.

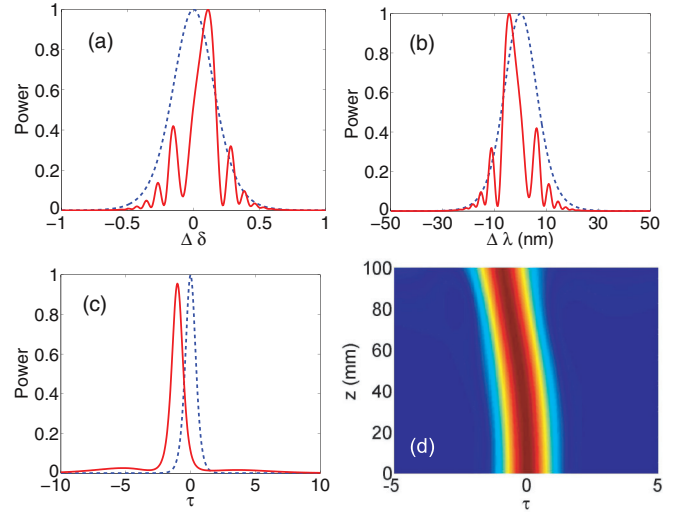


FIG. 3. (Color online) (a), (b) Input (dashed blue line) and output ($\xi = 5$, solid red line) power spectrum of a dissipative soliton with carrier wavelength $\lambda_0 = 1550$ nm and time duration $t_0 = 200$ fs for $g = 1$ and $g_2 = 0.04$ as a function of (a) dimensionless frequency and (b) physical wavelength. (c) Input (dashed blue line) and output ($\xi = 5$, solid red line) temporal DS profile. (d) Intensity counterplot of the spatiotemporal evolution of an accelerated dissipative soliton.

From the very beginning of the propagation, the pulse shape is perturbed by FCD and FCA and hence the approximate analytic treatment fails for long propagation distances. Figure 3 displays the effect of gain dispersion over the pulse propagation. Due to the finite bandwidth of the amplifying medium, the frequency shift is hampered after some saturation frequency (Ω_{sat}), as clearly predicted by our perturbative analysis:

$$\Omega(\xi) \simeq \Omega_{\text{sat}}(1 - e^{-\rho\xi}), \quad (17)$$

where

$$\Omega_{\text{sat}} = \frac{(\mu + \beta/2)\theta E^2}{10g_2(1 + \beta^2)}, \quad (18)$$

$$\rho = \frac{4}{3}g_2(1 + \beta^2)\eta^2. \quad (19)$$

Note that Ω_{sat} is directly proportional to FCD (μ) and inversely proportional to gain dispersion (g_2). Thus, $\Omega_{\text{sat}} \rightarrow +\infty$ as $g_2 \rightarrow 0$, meaning that practically no saturation is observed for broad amplifying windows. In order to solve the differential equation analytically, we approximate that the pulse energy remains conserved, which is strictly valid only for small propagation distances. Indeed, for long propagation distances, the pulse shape is significantly distorted by FC effects and the perturbative analysis fails to predict the evolution of the pulse parameters. Thus, in order to understand the carrier-induced pulse dynamics, we restrict our study to the limit of small propagation distance, where DSs approximately maintain their shape. In Figs. 3(a) and 3(b) we depict the input and output spectral power of a DS in the presence of gain dispersion, indicating that blueshift is reduced, as predicted by the theory. In Fig. 3(c) we show the temporal profile of a propagating pulse at $\xi = 5$ where the inherent background instability of DSs starts to affect the pulse propagation. The spatiotemporal

pulse evolution is displayed in Fig. 3(d), where the pulse acceleration is reduced by the effect of the gain dispersion.

In conclusion, we have provided a complete theoretical analysis of the carrier-induced DS dynamics in Si-based waveguides embedded in an amplifying medium. FCs generated through 2PA affect the refractive index of the medium and lead to a considerable self-frequency blueshift. We have derived analytical predictions based on soliton perturbative theory for the self-frequency blueshift

and for the temporal evolution. We have also examined the fully realistic condition where gain dispersion hampers the continuous spectral blueshifting, which is still observed. We have found that the saturation blueshifted frequency mainly depends on the amplifying window of the active medium.

This research was funded by the German Max Planck Society for the Advancement of Science (MPG).

-
- [1] B. Jalali, *J. Lightwave Technol.* **24**, 4600 (2006).
 - [2] J. Leuthold, C. Koos, and W. Freude, *Nat. Photonics* **4**, 535 (2010).
 - [3] L. Yin and G. P. Agrawal, *Opt. Lett.* **32**, 2031 (2007).
 - [4] Q. Lin, O. J. Painter, and G. P. Agrawal, *Opt. Express* **15**, 16604 (2007).
 - [5] C. Koos, P. Vorreau, T. Vallaitis, P. Dumon, W. Bogaerts, R. Beats, B. Esembeson, I. Biaggio, T. Michinobu, F. Diederich, W. Freude, and J. Leuthold, *Nat. Photonics* **3**, 216 (2009).
 - [6] A. W. Fang, H. Park, Y. Kuo, R. Jones, O. Cohen, D. Liang, O. Raday, M. N. Sysak, M. J. Paniccia, and J. E. Bowers, *Mater. Today* **10**, 28 (2007).
 - [7] L. Agazzi, J. Bradley, M. Dijkstra, F. Ay, G. Roelkens, R. Baets, K. Wörhoff, and M. Pollnau, *Opt. Express* **18**, 27703 (2010).
 - [8] N. Akhmediev and A. Ankiewicz, *Dissipative Soliton: Lecture Notes in Physics* (Springer, Berlin, 2005).
 - [9] A. Marini and D. V. Skryabin, *Phys. Rev. A* **81**, 033850 (2010).
 - [10] H. Rong, A. Liu, R. Nicolaescu, and M. Paniccia, *Appl. Phys. Lett.* **85**, 2196 (2004).
 - [11] Q. Lin, J. Zhang, G. Piredda, R. W. Boyd, P. M. Fauchet, and G. P. Agrawal, *Appl. Phys. Lett.* **91**, 021111 (2007).
 - [12] M. Dinu, F. Quochi, and H. Garcia, *Appl. Phys. Lett.* **82**, 2954 (2003).
 - [13] C.-J. Chen, P. K. A. Wai, and C. R. Menyuk, *Opt. Lett.* **19**, 198 (1994).
 - [14] D. Gomila, A. J. Scroggie, and W. J. Firth, *Physica D* **227**, 70 (2007).
 - [15] N. Akhmediev, J. M. Soto-Crespo, and G. Town, *Phys. Rev. E* **63**, 056602 (2001).
 - [16] B. A. Malomed and H. G. Winful, *Phys. Rev. E* **53**, 5365 (1996).
 - [17] A. Marini, D. V. Skryabin, and B. Malomed, *Opt. Express* **19**, 6616 (2011).
 - [18] M. F. Saleh, W. Chang, P. Hölzer, A. Nazarkin, J. C. Travers, N. Y. Joly, P. St. J. Russell, and F. Biancalana, *Phys. Rev. Lett.* **107**, 203902 (2011).
 - [19] G. P. Agrawal, *Nonlinear Fiber Optics*, 4th ed. (Academic Press, San Diego, 2007).
 - [20] H. Hasegawa and Y. Kodama, *Soliton in Optical Communication* (Oxford University Press, New York, 1995).
 - [21] C. A. Husko, S. Combrié, P. Colman, J. Zheng, A. De Rossi, and C. W. Wong, *Sci. Rep.* **3**, 1100 (2013).